

SHAPE REPRESENTATION AND A MORPHING SCHEME TO SUPPORT FLAPPING WING RESEARCH

Mohammad Sharif Khan and Tapabrata Ray

School of Engineering and Information Technology, University of New South Wales, Canberra 2610, Australia

Keywords: Flapping wing, Shape representation, Shape matching.

Abstract: Wing geometry is one of the most important factors that affects the performance of a flapping wing. The shape of insect wings and their nature of flapping varies across insect species. In order to gain an in-depth understanding of flapping flight with an aim to identify optimal wing shapes, there is a need for an universal and flexible shape representation scheme that is amenable to optimization. The paper presents a methodology to represent boundaries of insect wings which can be subsequently morphed via an optimization algorithm. The shapes are represented using B-splines, wherein the control points representing the shapes are repaired and subsequently evolved within an optimization framework. Twelve insect-wing shapes have been used to test the performance of the proposed method in the context of shape matching.

1 BACKGROUND

Research into flapping wings have gained significant attention in the last two decades (Donoughe et al., 2011; Nguyen et al., 2010). The wing area, wing span, aspect ratio, stiffness and flapping frequency are factors that are known to greatly influence the performance in terms of thrust and lift generation (Brugge-man, 2010).

In the context of flapping wing research, most of the papers attempt to study the effects of kinematics. There are only a small number of papers that have considered wing shapes (Altshuler et al., 2004; Phillips et al., 2010; Yuan et al., 2010; Ou and Jameson, 2011; Ou et al., 2011). An analysis of aerodynamic forces of revolving hummingbird wings and wing models is reported in (Altshuler et al., 2004), wherein the planform of the wing model was based on image of the left wing of a female ruby-throated hummingbird (*Archilochus colubris*) with a wing length of 46.5 mm and an aspect ratio of 7.72. An experimental investigation of the effects of planform on the flow structures generated by an insect-like flapping wing in hover is presented in (Phillips et al., 2010). Four planform shapes with a constant area and aspect ratio of approximately 6 were considered: reverse-ellipse, rectangle, four-ellipse and ellipse. Numerical simulations were performed in (Yuan et al., 2010) for a symmetrical NACA0005 airfoil in combined pitching-plunging motions at low

Reynolds numbers. Three-dimensional simulations of the two-dimensional airfoils with rectangular planform have been carried out with an Eppler61 airfoil and an oscillating NACA0012 airfoil at Reynolds number 46,000 and 40,000 respectively in (Ou and Jameson, 2011).

It is interesting to observe that in the field of flapping wing research, there is a move towards modeling insect like wing planforms with an aim to understand their effects on propulsive characteristics. The work outlined in this paper aims to provide a mechanism to represent and optimize wing shapes in order to understand the effects of wing shapes on the propulsive characteristics of a flapping flight. To this effect, we developed a flexible shape representation scheme. The flexible shape representation scheme when coupled with an optimization algorithm forms an useful tool that can be used to understand and answer why certain wing shapes have evolved within certain class of insects. It is important to highlight that both the efficiency of the optimization algorithm and the flexibility of shape representation scheme require serious attention. A lack of flexibility in shape representation will limit the evolution of various shapes, while an inefficient optimization algorithm will require evaluation of numerous shapes prior to its convergence, both of which are not desirable (Khan et al., 2011).

The boundary of a shape (such as a wing) can be represented using one of the following schemes: implicit polynomials (Landa et al., 2010), active con-

tours (Xu and Prince, 1998), cubic splines (Rogers and Adams, 1990), Bezier curves (Rogers and Adams, 1990) and B-spline curves (Cox, 1971; Riesenfeld, 1972). Among the above listed representations, B-spline curves have been most widely used as it ensures smoothness, compactness, local shape control, and affine transformation invariance (Mongkolnama et al., 2006). A B-spline representation has been used in the present study wherein the control points of the curve are identified through an optimization algorithm. A novel repair scheme is introduced and embedded to ensure generation of valid shapes (one without self intersection). The non-global behavior of B-spline curves makes it attractive in the realm of shape representation. The B-spline basis also allows the order of the basis function and hence the degree of the resulting curve to be changed without changing the number of defining polygon vertices (Rogers and Adams, 1990). Another advantage of the B-spline curve is its strong convex-hull property. It also possesses the variation diminishing and affine invariance properties.

In the context of shape matching, the aim is to identify a shape that is similar to a target shape. While methods based on active contours are commonly used in the field of pattern recognition (Xu and Prince, 1998), it must be highlighted that such methods use local information to update location of the points representing its boundary and hence not suitable for black-box optimization problems. In the current black-box application however, a single scalar error value (matching error) is only available to direct the search. In the present study, we assume that the length and the width of a common box enclosing all insect wings are known.

Rest of the paper is organized as follows. The method proposed in this paper is presented in Section 2. The results are reported in Section 3. Finally, some concluding remarks are provided in Section 4.

2 PROPOSED METHOD

In the proposed method, the number of control points required to represent the shape, the dimensions of the box enclosing the target shape and the centroid of the target shape are assumed to be known. The variables of the optimization problem are the x and y coordinates of the control points, the range of which are the same as the dimensions of the enclosing box. Every solution generated through the process of initialization or recombination is repaired, wherein the sequence of control points are changed to obtain a non-intersecting polygon net while maintaining the spe-

cific values of its coordinates. The concept is illustrated using Figure 1, 2 and 3, where the original randomly generated control polygon net and formation of the convex-hull are presented alongside its repaired form. Firstly, a convex-hull is generated using a set of control points (Figure 2). Thereafter, the points (lying inside the convex-hull) nearest to their adjacent edges are inserted to generate the non-intersecting control polygon net (Figure 3).

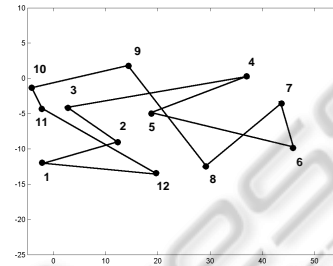


Figure 1: Position of initial control points without repair.

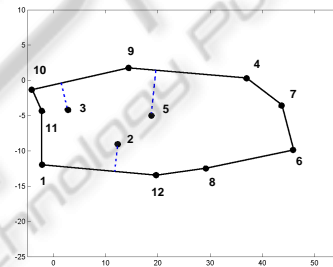


Figure 2: Convex-hull formation with initial control points.

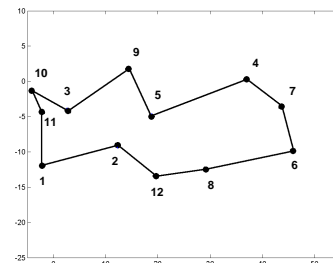


Figure 3: Position of initial control points after repair.

2.1 Initialization and Repair Strategy

The number of control points (N) used to describe a shape is a user defined parameter. Since the limits of x and y coordinates i.e. the space enclosing the target shape is known, a random solution is created and repaired during the phase of initialization.

2.2 Matching Error

Since the centroid of the target shape is known, the

shape generated using the repaired solution (re-ordered set of control points) is shifted such that its centroid matches the centroid of the target shape. The maximum of Euclidean and Hausdorff distance is computed using the generated shape and the target shape.

2.3 Optimization Algorithm

2.3.1 Evolution

The pseudo-code of the proposed optimization is presented in Algorithm 1 and 2. In the proposed algorithm, two different evolution strategies are used for generating the offspring population. These are:

Algorithm 1: Proposed algorithm.

- 1: pop_1 = Initialize {Assumption of number of control points}
 - 2: pop_1 = Repair (pop_1) {Maintaining the sequence of control points considered as variables}
 - 3: CP_n = Centroid_Shift (s_T, s_G) {Shifting of control points towards a particular distance measured with the difference between the centroids of target and generated shapes}
 - 4: E_dist = Max (Eucli_dists (s_T, s_G))
 - 5: H_dist = Hausdorff_dist (s_T, s_G)
 - 6: $Matching_Error$ = Max (E_dist, H_dist)
 - 7: Hybrid Memetic Algorithm presented in Algorithm 2
-

1. *EA-like evolution* – This includes simulated binary (SBX) crossover and polynomial mutation (Deb and Agarwal, 1995).
2. *DE-like evolution* – This includes the DE exponential crossover and mutation, as described in (Das and Suganthan, 2010).

2.3.2 Ranking and Reduction

Since the test problems studied in the paper are formulated as single-objective, unconstrained minimization problems, the ranking is done by sorting the objective values in ascending order. The best N solutions from the (parent+child) population form the population for the next generation.

2.3.3 Local Search

At each generation, in addition to generation of new solutions using recombination and mutation, a local search is used for further improvement. Sequential quadratic programming (SQP) (Powell, 1978) is used for the local search in the present study. After perfor-

Algorithm 2: Hybrid memetic algorithm.

Require: Population size (N), Number of generations (N_G), Crossover and mutation parameters.

- 1: pop_1 = Initialize
 - 2: pop_1 = Repair (pop_1)
 - 3: Evaluate (pop_1)
 - 4: **for** $i = 2$ to N_G **do**
 - 5: **if** rand (0,1) \leq 0.5 **then**
 - 6: $childpop_i$ = Evolve_EA (pop_{i-1})
 - 7: **else**
 - 8: $childpop_i$ = Evolve_DE (pop_{i-1})
 - 9: **end if**
 - 10: $childpop_i$ = Repair ($childpop_i$)
 - 11: Evaluate ($childpop_i$)
 - 12: S = Rank ($pop_{i-1} + childpop_i$)
 - 13: **if** rand (0,1) \leq 0.2 **then**
 - 14: \mathbf{x} = Random_x $\in pop_i$ {Select a random solution}
 - 15: **else**
 - 16: \mathbf{x} = Choose_start_x (pop_i) {Select a solution as described in Section 2}
 - 17: **end if**
 - 18: \mathbf{x}_{best} \leftarrow Local_search (\mathbf{x}) { \mathbf{x}_{best} is the best solution found using local search from \mathbf{x} }
 - 19: Replace worst solution in pop_i with \mathbf{x}_{best}
 - 20: pop_i = Rank(pop_i) {Rank the solutions again in pop_i }
 - 21: **if** local search doesn't improve the objective value for K consecutive generations **then**
 - 22: pop_i = Re-initialize () {Retain the best solution while re-initializing}
 - 23: pop_i = Repair (pop_i)
 - 24: **end if**
 - 25: **end for**
-

ming the local search, the worst solution in the population is replaced by the best solution found from the local search.

2.3.4 Re-initialization

In order to prevent the algorithm from stagnating at a local optima, the population is reinitialized if there is no improvement observed in the objective value for more than K (=10) generations. The best solution found during the search is preserved in the population during re-initialization.

3 RESULTS

The boundaries of the wings are extracted digitally and then target shapes are obtained via direct inverse

Table 2: Matching error between target and generated dragonfly-wing shapes.

Dragonfly wing	wing-1	wing-2	wing-3	wing-4	wing-5	wing-6	wing-7
Matching error (proposed method)	6.4e-05	1.8e-05	1.9e-04	2.3e-05	3.8e-05	7.1e-05	2.2e-05
Matching error (real-coded EA)	4.019	3.670	2.747	3.850	5.071	5.388	3.854

Table 3: Matching error between target and generated damselfly-wing shapes.

Damselfly wing	wing-1	wing-2	wing-3	wing-4	wing-5
Matching error (proposed method)	2.1e-04	2.9e-05	7.1e-04	0.9e-05	3.3e-05
Matching error (real-coded EA)	3.466	5.849	4.545	3.833	2.562

Table 4: Results of multiple runs for dragonfly-wing and damselfly-wing shapes using proposed method.

Shapes	Error Measurement	Best	Worst	Mean	Median	Std.
Dragonfly-wing-1	Max(Eucli,HD)	0.7e-05	1.57e-04	5.0e-05	3.3e-05	4.0e-05
Dragonfly-wing-5	Max(Eucli,HD)	0.9e-05	2.11e-04	5.2e-05	1.8e-05	6.9e-05
Damselfly-wing-2	Max(Eucli,HD)	0.8e-05	3.3e-04	6.2e-05	2.7e-05	8.9e-05
Damselfly-wing-5	Max(Eucli,HD)	0.7e-05	1.73e-04	4.0e-05	2.9e-05	3.6e-05

Table 5: Results of multiple runs for dragonfly-wing and damselfly-wing shapes using real-coded Evolutionary Algorithm.

Shapes	Error Measurement	Best	Worst	Mean	Median	Std.
Dragonfly-wing-1	Max(Eucli,HD)	1.763	8.796	4.894	4.395	1.823
Dragonfly-wing-5	Max(Eucli,HD)	2.813	8.085	4.663	4.034	1.686
Damselfly-wing-2	Max(Eucli,HD)	3.540	6.402	5.097	5.344	0.815
Damselfly-wing-5	Max(Eucli,HD)	2.219	6.255	3.719	3.453	1.066

Table 1: Parameters used for the proposed algorithm.

Parameter	Value
Population size	40
Max. function evaluations	10000
Crossover probability	1.0
Crossover index	10
Mutation probability	0.05
Mutation index (polynomial)	20
Scale factor F (for DE mutation)	0.9

fitting in order to remove noise from their boundaries (Figure 4). Seven dragonfly-wing shapes and five damselfly-wing shapes are used to test the performance of the proposed approach. Dragonfly-wing shapes contain 493 to 525 points while Damselfly-wing shapes contain 491 to 516 points. The parameters used for the algorithms are the same for each shape matching exercise, i.e., no tuning of parameters is done across the problems. The parameters are listed in Table 1. A maximum of 10000 function evaluations are set for each problems.

For all the problems, we have assumed they can be represented using 20 control points which translates to a 40 variable optimization problem. A common

box has been chosen as the search domain representing between 0 to 58 in the x direction and between 0 to 17 in the y direction for all the problems. The results after 10000 function evaluations for dragonfly-wing and damselfly-wing shapes are shown in Table 2 and Table 3 respectively. For the sake of comparison, the results of using a real-coded evolutionary algorithm are also presented alongside the results of the proposed method.

The statistics of the multiple runs of some examples are presented in Table 4, which reflects the consistency of the proposed approach. The best and worst values are reported as the minimum and maximum errors across 20 runs, respectively. The median value reported is the average of 10th and 11th values in the sorted list of matching errors obtained across 20 runs. The matching errors for all the examples are fairly low in the order of $1e^{-05}$. In an attempt to observe the performance of the proposed method, the results of the multiple runs of using a real-coded evolutionary algorithm are also presented in Table 5. It is clear from Table 4 and Table 5, that a significant improvement in performance has been achieved through the

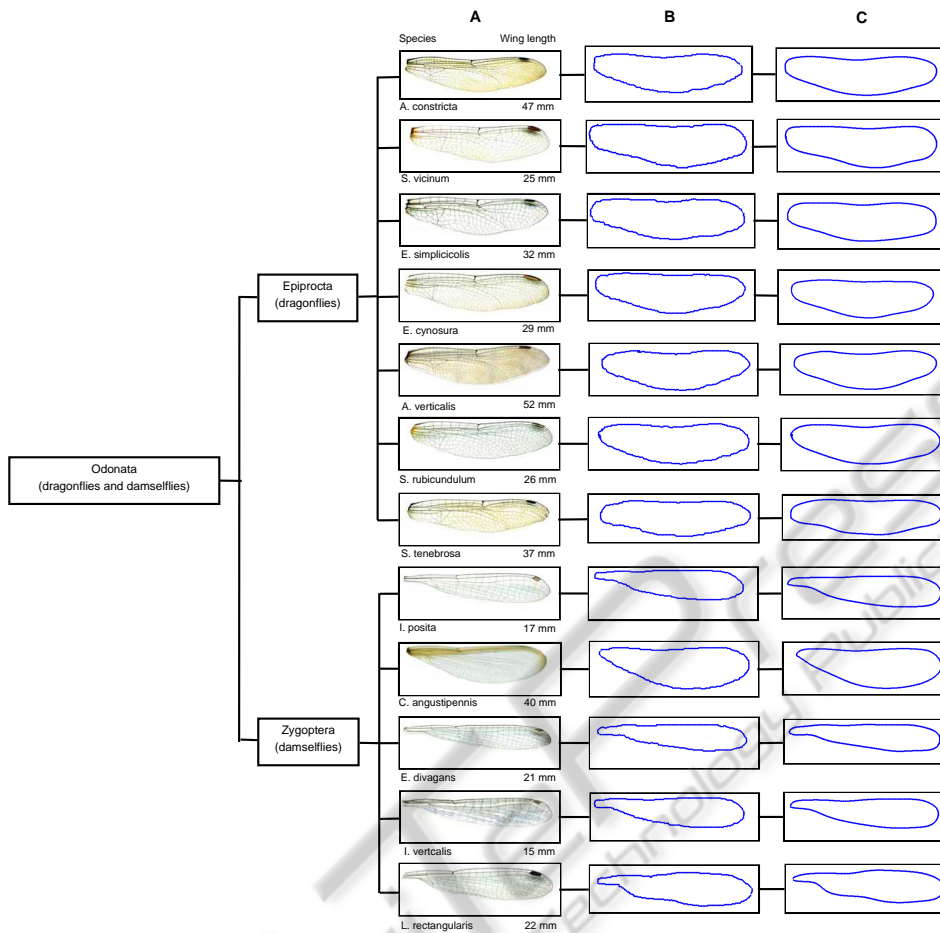


Figure 4: **A:** Dragonfly and damselfly wing species with their length (Donoughe et al., 2011). **B:** Original shapes' boundaries (digitized) of wing species. **C:** Shapes' boundaries are represented via direct inverse fitting.

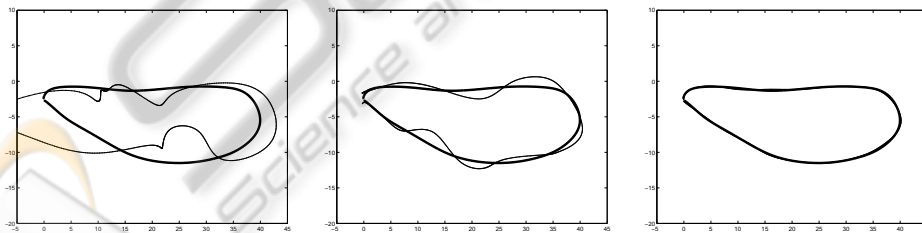


Figure 5: Evolutions of generated damselfly-wing-2 (thin) towards the target damselfly-wing-2 (thick) for matching.

use of the proposed method across all the problems. Various states of evolutions (from 1 to 10000 function evaluations in 3000 interval) of generated shape towards the target or original shape are shown in Figure 5 for damselfly-wing-2 example.

4 DISCUSSION AND CONCLUSIONS

There is an increasing interest to understand flapping behavior of insect wings with an aim to identify efficient propulsive mechanisms for micro air vehicles. While flapping wing kinematics have been the primary focus for the last decade, there are increasing number of attempts in recent years that tend to model

insect like wing planforms. This paper presents a boundary shape representation scheme coupled with a novel repair method that is amenable to optimization. The ability of the approach to represent and morph a class of insect wings is illustrated through shape matching, wherein the entire class of insect wing shapes have been identified using a common bounding frame. The approach relies on the use of B-splines for shape representation, in which the control points are ordered using a repair strategy. The repair strategy assists in generating more viable shapes, thereby increasing the rate of convergence in the optimization exercise. In an attempt to enhance the convergence further, a memetic algorithm embedded with a local search based on SQP is designed. In order to measure the matching error between the target shape and generated shape, two popular similarity measures (Euclidean and Hausdorff distance) have been considered. The proposed method has been tested using seven dragonfly-wing and five damselfly-wing shapes, wherein a good performance has been obtained. It is important to highlight that although this study focused on shape matching, i.e. by considering the objective as a similarity measure, other objectives such as propulsive efficiency, lift or drag can be easily included in the formulation of the optimization problem provided they can be computed automatically without user intervention.

REFERENCES

- Altshuler, D. L., Dudley, R., and Ellington, C. P. (2004). Aerodynamic forces of revolving hummingbird wings and wing models. *Journal of Zoology*, 264(4):327332.
- Bruggeman, B. (2010). Improving flight performance of delfly II in hover by improving wing design and driving mechanism. Master's thesis, Faculty of Aerospace Engineering, Delft University of Technology.
- Cox, M. (1971). The numerical evaluation of B-splines. *IMA Journal of Applied Mathematics*, 4(10):134–149.
- Das, S. and Suganthan, P. (2010). Differential evolution: A survey of the state-of-the-art. *IEEE Transactions on Evolutionary Computation*, 99:1–28.
- Deb, K. and Agarwal, S. (1995). Simulated binary crossover for continuous search space. *Complex Systems*, 9:115–148.
- Donoughe, S., Crall, J. D., Merz, R. A., and Combes, S. A. (2011). Resilin in dragonfly and damselfly wings and its implications for wing flexibility. *Journal of Morphology*.
- Khan, M. S., Ayob, A. F. M., Isaacs, A., and Ray, T. (2011). A smart repair embedded memetic algorithm for 2D shape matching problems. *Engineering Optimization*.
- Landa, Z., Malah, D., and Barzohar, M. (2010). 2D object description and recognition based on contour matching by implicit polynomials. In *proceedings of the 18th European Signal Processing Conference*.
- Mongkolnana, P., Dechsakulthorn, T., and Nukoolkita, C. (2006). Image shape representation using curve fitting. In *Proceedings of the 6th WSEAS International Conference on Signal, Speech and Image Processing*, Lisbon, Portugal.
- Nguyen, Q., Parki, H., Byun, D., and Goo, N. (2010). Recent progress in developing a beetle-mimicking flapping-wing system. In *World Automation Congress*.
- Ou, K., Castonguay, P., and Jameson, A. (2011). 3D flapping wing simulation with high order spectral difference method on deformable mesh. In *49th AIAA Aerospace Sciences Meeting including the New Horizons Forum and Aerospace Exposition*, Orlando, Florida.
- Ou, K. and Jameson, A. (2011). Towards computational flapping wing aerodynamics of realistic configurations using spectral difference method. In *20th AIAA Computational Fluid Dynamics Conference*, Honolulu, Hawaii.
- Phillips, N., Knowles, K., and Lawson, N. J. (2010). Effect of wing planform shape on the flow structures of an insect-like flapping wing in hover. In *27th International Congress of The Aeronautical Sciences*.
- Powell, M. (1978). *A fast algorithm for nonlinearly constrained optimization calculations*, volume 630/1978. SpringerLink.
- Riesenfeld, R. (1972). *Application of B-spline approximation to geometric problems of computer aided design*. PhD thesis, Syracuse University.
- Rogers, D. and Adams, J. (1990). *Mathematical elements for computer graphics*. McGraw-Hill.
- Xu, C. and Prince, J. L. (1998). Snakes, shapes, and gradient vector flow. *IEEE Transactions on Image Processing*, 7(3).
- Yuan, W., Lee, R., Hoogkamp, E., and Khalid, M. (2010). Numerical and experimental simulations of flapping wings. *International Journal of Micro Air Vehicles*, 2(3):181–208.